Journal of Catalysis **207,** 317–330 (2002)
doi:10.1006/jcat.2002.3556, available online at http://www.idealibrary.com on IDEAL®

Acetic Acid Reduction by H_2 over Supported Pt Catalysts: A DRIFTS and TPD/TPR Study

Willy Rachmady and M. Albert Vannice[1]

Department of Chemical Engineering, Pennsylvania State University, University Park, Pennsylvania 16802-4400

Received October 2, 2001; revised February 4, 2002; accepted February 4, 2002

The utilization of DRIFTS combined with TPD and TPR experiments resulted in the identification of molecular acetic acid, acyl species, and bidentate acetate species present on the titania surface plus CO adsorbed on Pt following acetic acid adsorption on Pt/TiO_2 catalysts at 300 K. TPR studies in the presence of H_2 provided evidence that reduction of acetic acid on TiO_2-supported Pt begins via a reaction between adsorbed H atoms from the Pt surface and an acyl species on titania, and this pathway serves as the major route for production of acetaldehyde, which can be further hydrogenated to ethanol. The stability of the acetate species under the steady-state reaction conditions employed here discounts it as an active intermediate; however, at temperatures above 500 K these acetate groups may also become reactive intermediates to form acetaldehyde. The absence of both surface acyl species and stable acetate species on Pt/SiO_2 accounts for the lack of reduction activity on this catalyst and explains why only decomposition products were formed. Based on this new spectroscopic information, a reaction mechanism proposed recently was modified slightly to incorporate an acyl species as the principal intermediate, rather than molecular acetic acid, and the resulting rate expression not only gives an identical fit to the kinetic data, but also possesses thermodynamically meaningful parameters, such as the heat of adsorption of H_2 on Pt, that are consistent with literature values.

INTRODUCTION

Understanding the mechanistic details of a reaction at the molecular level can be an integral part of designing and developing better catalysts. Insight into the sequence of steps comprising a catalytic reaction can be acquired by carefully relating the macroscopic behavior, such as activity and selectivity, to observations acquired from spectroscopic studies of molecular species. This method is often problematic because of the different conditions used in the spectroscopic techniques compared to practical reaction conditions; however, *in situ* spectroscopic studies allow researchers to obtain information at the molecular level at, or near, actual reaction conditions. In particular, infrared spectra acquired *in situ* can identify species present on the catalyst surface, while temperature-programmed desorption (TPD) and temperature-programmed reaction (TPR) allow an examination of the stability and the reactivity of these species. These techniques were employed here to develop a better fundamental understanding of the reactions between hydrogen and organic acids.

The reaction between acetic acid and H_2 was chosen as a probe representative of aliphatic carboxylic acid reduction over supported metal catalysts because of its simplicity and the importance of a direct route to catalytically reduce organic acids with H_2 (1). A better understanding of this reaction could lead to an improved method to synthesize industrially important chemicals, such as aldehydes, alcohols, and esters, from renewable, relatively cheap carboxylic acids. Several active intermediates have been proposed for this series of hydrogenation/hydrogenolysis reactions, including molecular acetic acid and its dissociated forms; however, there is no direct evidence to verify the kinetic role of any of these surface species. This is mainly due to a lack of adequate techniques to identify active intermediates during a reaction. Consequently, because of this uncertainty, mechanistic details have been open for debate.

A model based on a Langmuir–Hinshelwood-type mechanism has been proposed to describe the kinetics of acetic acid hydrogenation on Pt/TiO_2 catalysts, and it invoked molecular acetic acid adsorbed on the TiO_2 surface as a catalytically significant species (1). On the other hand, Pei and Ponec have proposed an acetate species as an active intermediate in their study of this reaction on oxides because this surface species was observed on all active catalysts (2). However, this assignment of acetate as a principal intermediate was based solely on its presence on the catalyst surface, as indicated by infrared data, and no distinction was made between a spectator species versus an active reaction intermediate. Dumesic and coworkers proposed acyl species as an active intermediate in this reaction over supported Cu catalysts, which was a conclusion derived from the ease of formation of acyl species during ester adsorption in a reducing environment (3). However, the authors did point out that the mechanism by which acetic acid reduction takes place could be different from that of esters because acyl species are easier to form from esters than from carboxylic acids.

[1] To whom correspondence should be addressed. E-mail: mavche@engr.psu.edu.

0021-9517/02 $35.00

Pestman has suggested that acetic acid hydrogenation proceeds via a Mars–van Krevelen-type mechanism, in which the surface, in this case a partially reduced oxide surface, takes part in the reaction by adsorbing acetic acid at an oxygen vacancy and abstracting an oxygen atom, thereby producing acetaldehyde (4); thus the role of the oxide is to reduce the acetic acid molecule. This oxygen atom is then removed by hydrogen. An isotope-labeling study supported the proposal, but it could not exclude the possibility that the reaction may also proceed via a Langmuir-type mechanism, in which a reaction occurs between adsorbed acetic acid and adsorbed hydrogen.

The present study used DRIFTS combined with TPD and TPR to examine the nature of these adsorbed species and their role in the reaction, and the results indicate that molecular acetic acid as well as surface acyl and acetate species can be present on the surface of Pt/TiO_2 catalyst under reaction conditions. Their relative stability and reactivity dictate their importance in the catalytic cycle describing the hydrogenation reaction.

EXPERIMENTAL

Adsorption of acetic acid, acetaldehyde, and ethanol on 2% Pt/TiO_2 and 0.7% Pt/SiO_2 was examined. The preparation, pretreatment, and characterization of these catalysts were described in detail in a previous publication (1). Before use in any experiment, 2.01% Pt/TiO_2 was reduced *in situ* in flowing H_2 (1 atm) at either 473 K for 2 h, which is referred as low-temperature reduction (LTR), or 773 K for 1 h, which is referred as high-temperature reduction (HTR). The 0.68% Pt/SiO_2 catalyst was reduced in flowing H_2 at 723 K for 1 h.

DRIFTS (diffuse reflectance infrared Fourier transform spectroscopy) was used to examine the nature of the adsorbed species on the catalysts. The system consisted of an FTIR spectrometer (Mattson Instrument, RS-1000) equipped with a DRIFTS cell (Harrick Scientific, HVC-DR2) and a praying mantis mirror assembly (Harrick Scientific, DRA-2-CO) which had been modified to allow catalyst pretreatment, as well as reactions, to be conducted *in situ* (5). Infrared spectra of adsorbed species were collected at atmospheric pressure and temperatures from 298 to 473 K at a resolution of 4 cm^{-1}. Each spectrum after adsorption was referenced to that of the freshly pretreated sample just prior to introduction of the adsorbate. Although these spectra are represented here in absorbance units, they were also plotted in Kubelka–Munk units, which gave very similar spectra (not shown here).

Temperature-programmed desorption (TPD) and temperature-programmed reaction (TPR) experiments were conducted using a glass microreactor equipped with a quadrupole mass spectrometer for monitoring the desorption of surface species. Up to 15 mass numbers were simultaneously monitored during each run, and their respective signal intensities were recorded and reported without correction for sensitivity factors. The desorption curve for each compound was traced by following (but was not limited to) the mass numbers listed in Table 1. The heating rate was 20 K/min using 50 cm^3 (STP)/min He in the TPD runs or 50 cm^3 (STP)/min H_2 in the TPR runs as the carrier gas. The absence of concentration gradients and significant lag times in the sample cell as well as the absence of diffusion limitations in the pores was verified using criteria described by Gorte (6). Acetic acid (Glacial 99.7%, E.M. Science), acetaldehyde (99.9%, Aldrich), and ethanol (99.9%, Aldrich) were degassed before use by subjecting them to freeze–thaw cycles in an inert atmosphere and the vapor was introduced into the DRIFTS cell or microreactor by using a saturator and passing the carrier gas through a bubbler in each liquid.

TABLE 1

Assignment of Mass Numbers Detected by Mass Spectroscopy

Compound	Mass number (amu)
Acetic acid	15, 45, 60
Acetaldehyde	29, 44
Ethanol	31
Acetone	43, 58
Ethylene	27
Ketene	14, 41, 42
CH_4	15, 16
CO	28
CO_2	44
H_2	2

RESULTS

DRIFTS and TPD of Acetic Acid on Pt/TiO_2

Infrared spectra of species resulting from acetic acid adsorption on Pt/TiO_2 were obtained after flowing acetic acid vapor (2 Torr) through the DRIFTS cell for 30 min, followed by purging the cell for 1.5 h with flowing argon or helium maintained at atmospheric pressure and 303 K during this process. Figure 1 shows infrared spectra after adsorption of acetic acid on Pt/TiO_2 and Pt/SiO_2 catalysts, and three different surface species can be identified—acyl, acetate, and adsorbed CO. The surface acyl species is characterized by a band at 1680 cm^{-1} for ν(C=O), surface acetate by bands at 1450 cm^{-1} for ν_s(COO) and 1540 cm^{-1} for ν_a(COO), and adsorbed CO by a band at 2065 cm^{-1}. A complete list of infrared band assignments is given in Table 2 (7–10, 13–25). Both acyl and acetate species were formed on the titania surface, as identical bands were observed during acetic acid adsorption on pure titania. On the other hand, CO was adsorbed on Pt, as characterized by a band near 2050 cm^{-1} (7, 8). The stronger absorption

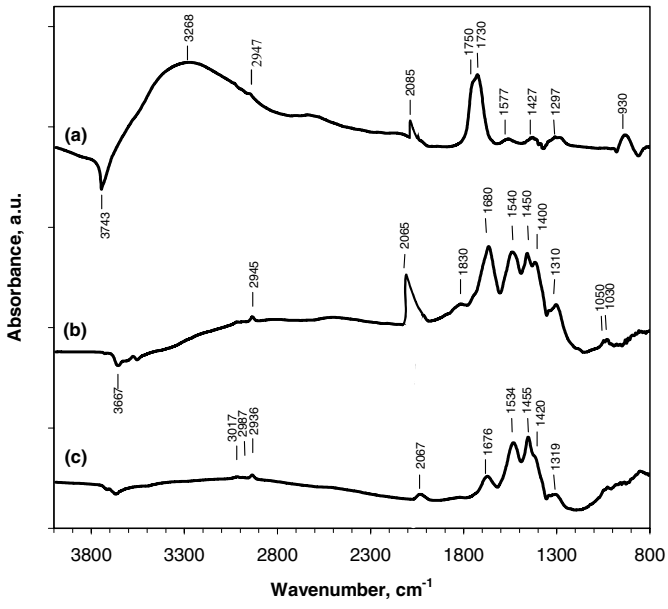

FIG. 1. DRIFT spectra of surface species formed following adsorption of acetic acid on: (a) 0.7% Pt/SiO_2, (b) 2% Pt/TiO_2 (LTR), and (c) 2% Pt/TiO_2 (HTR).

intensity of this band on the LTR catalyst relative to that on the HTR catalyst indicates a higher CO concentration on the LTR catalyst, which was expected because some of the Pt surface was covered by titania in the HTR catalyst (9).

Acetate can be bound to the surface in a monodentate, a bidentate, or a bridging configuration (10). The monodentate configuration is characterized by a splitting of the carboxylate stretching frequencies, namely ν_s(COO) and ν_a(COO), that is much greater than that of an ionic complex ($\sim$160 cm^{-1}). In this configuration, the acetate is bound to the surface through only one of its oxygen atoms. The bidentate configuration, alternatively, is characterized by a splitting of the carboxylate stretching frequencies, which is significantly less than the ionic value, and the acetate is bound to the surface via both oxygen atoms linked to one metal cation. Finally, the bridging configuration is characterized by a splitting larger than that of the bidentate, yet close to the ionic value, and the acetate is bound to the surface with the two oxygen atoms bound to two metal sites. Thus, we can associate the bands at 1540 and 1450 cm^{-1} with acetate in the bidentate configuration, which is consistent with previous work (2).

The acyl species is weakly adsorbed on the catalysts, as it is not detected at high temperatures. The relative amount of this species is also larger on the less reduced titania surface, as shown by the infrared spectrum obtained for the LTR catalyst. Furthermore, the intensity of the infrared band associated with acyl species decreased as the degree of reduction increased, as observed in experiments conducted on titania with various degrees of reduction (26).

There is no evidence that molecular acetic acid is present on the surface following the purge to remove acetic acid vapor from the cell. In the presence of vapor-phase acetic acid, however, a band at 1725 cm^{-1} exists with both TiO_2 and Pt/TiO_2 and appears in the spectrum after the gas-phase contribution is subtracted. This band is assigned to

TABLE 2

Vibrational Mode Assignments for Surface Species Following Acetic Acid Adsorption at 300 K

Band	Infrared band wavenumber (cm^{-1})					
	$CH_3COOH_{(g)}$ [a]	$CH_3COOH_{(s)}$ [b]	Pt/SiO_2	Pt/TiO_2 (LTR)	Pt/TiO_2 (HTR)	Ref.
ν(OH)	3583	2875	3268			13
$\nu(CH_3)$			3032	3016	3017	
			2990	2986	2987	14
			2947	2936	2936	
ν(C=O), Pt–CO (linear)			2085	2065	2067	7, 8, 15
ν(C=O), Pt–CO (bridging)				1830	1822	7, 8, 15
ν(C=O), silyl ester			1750			16
ν(C=O), acetic acid	1788	1648	1730			13
ν(C=O), acyl				1680	1676	17–23
ν_a(COO), acetate			1577	1540	1534	10, 14
ν_s(COO), acetate			1427	1450	1455	9, 14
$\delta(CH_3)$	1395	1439		1400	1420	24
ν(C–O), acetic acid	1178	1284	1297	1310	1319	
δ(OH)	1280	1418				
$\rho(CH_3)$	988	1049		1050	1050	
				1030	1030	
γ(OH)		923	930			25
ν(C–C)		908				

[a] From Ref. (11).
[b] From Ref. (12).

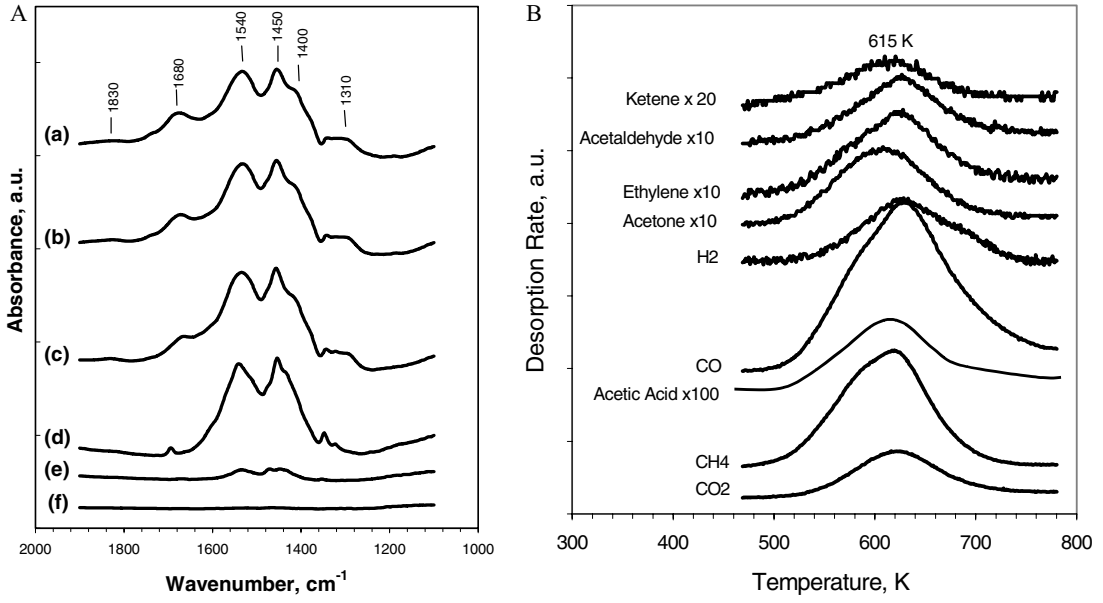

FIG. 2. (A) DRIFT spectra of species adsorbed on Pt/TiO_2 (HTR) after stepwise heating in Ar to (a) 300, (b) 373, (c) 473, (d) 573, (e) 673, and (f) 773 K. (B) TPD spectra following acetic acid adsorption on Pt/TiO_2 (HTR) at 300 K.

adsorbed molecular acetic acid because it falls into the region of carbonyl stretching frequencies ν(C=O) for constrained acetic acid (13).

For TPD experiments, the catalyst surface was saturated by exposure to acetic acid vapor and then purged at room temperature in a procedure identical to that applied in the DRIFTS experiments. TPD spectra of surface species following acetic acid adsorption on Pt/TiO_2 (LTR) and Pt/TiO_2 (HTR) show no observable peaks at temperatures below 500 K, as shown in Figs. 2B and 3B; however, well-developed peaks occur between 500 and 700 K. There is no desorption of acetic acid at lower temperatures, which confirms the DRIFTS results that purging the catalysts at 300 K eliminates weakly chemisorbed molecular acetic acid from the surface. The disappearance of the band at 1680 cm^{-1} in the infrared spectrum for Pt/TiO_2 (LTR) after heating to 573 K occurs concomitantly with the desorption of ketene (41 amu), which has a TPD peak at 573 K. The desorption of ketene at this temperature is consistent with the assignment of the 1680 cm^{-1} band to surface acyl species

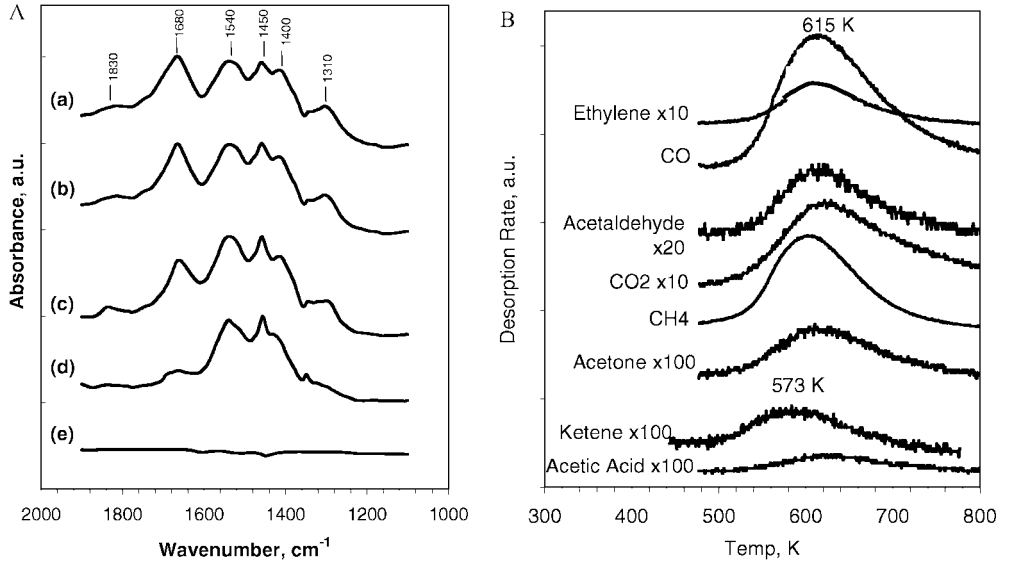

FIG. 3. (A) DRIFT spectra of species adsorbed on Pt/TiO_2 (LTR) after stepwise heating in Ar to (a) 300, (b) 373, (c) 473, (d) 573, and (e) 673 K. (B) TPD spectra following acetic acid adsorption on Pt/TiO_2 (LTR) at 300 K.

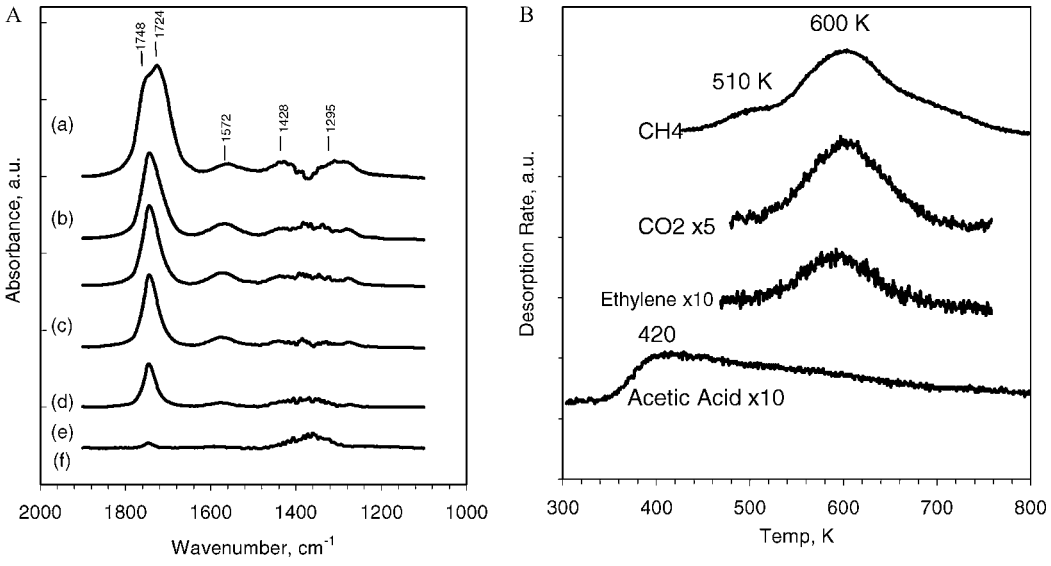

FIG. 4. (A) DRIFT spectra of species on Pt/SiO_2 following acetic acid adsorption at 300 K and heating in Ar to (a) 300, (b) 373, (c) 473, (d) 573, (e) 673, and (f) 773 K. (B) TPD spectra following acetic acid adsorption on Pt/SiO_2 at 300 K.

because ketene is expected to be easily produced during decomposition of such groups. Based on the DRIFT spectra of surface groups after stepwise heating to 773 K, as displayed in Figs. 2A and 3A, bidentate acetate species mostly decompose between 573 and 673 K. The TPD peaks above 573 K must then be the result of a transformation of acetate species at these temperatures due to either acetate decomposition or surface reactions involving acetate and/or its decomposition products.

The desorption peaks of species adsorbed on Pt/TiO_2 (HTR) (see Fig. 2B) are dominated by fragmentation products such as methane (16 amu), CO (28 amu), CO_2 (44 amu), and H_2 (2 amu). Traces of acetic acid (45 amu) also desorbed around 610 K. Other C_2 species desorbed between 573 and 673 K were acetaldehyde (29 amu), ethylene (27 amu), and ketene (41 and 42 amu), and acetone (43 amu) was also detected. The water peak was unresolved with both the LTR and HTR catalysts and there was no evidence for ethanol formation on either catalyst.

DRIFTS and TPD of Acetic Acid on Pt/SiO_2

After adsorption of acetic acid, the surface of Pt/SiO_2 was predominantly covered by silyl esters and molecular acetic acid interacting with surface hydroxyl groups. An IR spectrum of species present on Pt/SiO_2 (Fig. 1) showed a band at 1730 cm^{-1} with a shoulder at 1750 cm^{-1}. The latter is characteristic of ν(C=O) for silyl esters formed by dissociative acetic acid adsorption on a SiO_2 surface (16), and the former can be assigned to ν(C=O) in hydrogen-bonded molecular acetic acid. The band at 930 cm^{-1} is a result of an out-of-plane vibration of the O–H bond in adsorbed acetic acid (25). The broad band at 3268 cm^{-1} reconfirms that acetic acid is adsorbed on a SiO_2 surface via hydrogen bonding. The interaction of the lone electron pair of the carbonyl oxygen atom in acetic acid with hydrogen in the free hydroxyl groups on silica causes a large shift in the free OH bands, ν(O–H), toward lower frequencies; consequently, there is a loss of intensity in the infrared absorption band at 3743 cm^{-1} of the free hydroxyl groups, as is apparent in the spectrum. Finally, a large red shift in the ν(C=O) frequency for adsorbed molecular acetic acid is consistent with hydrogen bonding through its carbonyl oxygen to a hydroxyl group. Very weak bands appear at 3032, 2990, and 2947 in Fig. 1a that result from the ν(C–H) vibrations of adsorbed molecular acetic acid (26). All band assignments are listed in Table 2.

Strong IR absorption at 2085 cm^{-1} and a shoulder at 2023 cm^{-1} are indicative of CO adsorbed on Pt, and as the catalyst was heated, the band intensities grew stronger and reached a maximum near 473 K. A dip in the 2065 cm^{-1} band resulted from the presence of residual CO on Pt even before acetic acid was introduced, which is an effect similar to that observed with Pt/TiO_2 catalysts. Bands at 1577 and 1427 cm^{-1} can be assigned to surface acetate species and, because such bands were not observed with acetic acid adsorption on SiO_2 alone, the species are presumed to be on Pt. Temperature-programmed desorption after acetic acid adsorption on Pt/SiO_2 showed three groups of peaks, at 420, 510, and 600 K (Fig. 4B). Peaks at 400 K can be interpreted as fragmentation products of adsorbed molecular acetic acid, which is consistent with both the disappearance of the IR band at 1724 cm^{-1} upon heating to 373 K in the DRIFTS experiment and the assignment of the band at 1724 cm^{-1} to weakly bonded acetic acid. The intermediate peaks at 500 K consist only of amu values of 14, 15, and

16, which indicate methane desorption at this temperature. At 600 K, besides being dominated by methane desorption, smaller amounts of CO_2 (44 amu) and ethylene (27 amu) were observed which were associated with the decomposition of silyl esters.

DRIFTS and TPD of Acetaldehyde on Pt/TiO_2 (HTR)

Because acetaldehyde and ethanol are products of acetic acid hydrogenation over Pt/TiO_2, their adsorption behavior on the catalyst is of importance to better understand the mechanistic details of the reaction. Acetaldehyde adsorption on Pt/TiO_2 produced bands characteristic of adsorbed molecular acetaldehyde, crotonaldehyde, surface acyl species, acetate, and CO, as shown in Fig. 5A. Complete band assignments are in Table 3 (7–10, 15, 22, 23, 27, 30, 34). Crotonaldehyde results from acetaldehyde aldolization, which is expected on TiO_2 surfaces (27–29). By comparison to previous spectroscopic studies (27, 30), adsorbed crotonaldehyde is indicated by IR bands at 3023 cm^{-1} for ν(C=C–H), 1655 cm^{-1} for ν(C=O), 1606 cm^{-1} for ν(C=C), 1377 cm^{-1} for $\delta(CH_3)$, and 1141 cm^{-1} for $\rho(CH_3)$ or ν(C–C). A shoulder at 1680 cm^{-1}, which was more apparent after the catalyst was heated to 373 K, can be ascribed to surface acyl species. An IR band at 1630 cm^{-1}, which also became apparent after heating to 373 K, is assigned to a bending mode of adsorbed molecular water, which is supported by the appearance of a very broad band resulting from the hydroxyl stretching vibrations at 3450 cm^{-1} (31). Bands at 1550 and 1442 cm^{-1} undoubtedly belong to acetate species on titania and are identical to those formed during acetic acid adsorption on the same catalysts. This result indicates that acetaldehyde is oxidized to acetate during chemisorption, which is behavior similar to that observed with tin(IV) oxide (32). CO formation on Pt as a result of acetaldehyde decarbonylation is also evidenced by an IR band at 2041 cm^{-1}.

TPD spectra of species following acetaldehyde chemisorption on Pt/TiO_2 (HTR) showed that molecular acetaldehyde and ketene desorbed around 380 K (see Fig. 5B). The next group of peaks around 623 K was dominated by signals from CO and H_2 along with much smaller amounts of CH_4, CO_2, and acetone. There was no detectable signal for amu values of 29, 41, and 42, thus indicating the absence of acetaldehyde and ketene desorption at this temperature. No crotonaldehyde desorption from the

TABLE 3

Vibrational Assignments for Surface Species Following Acetaldehyde Adsorption on Pt/TiO_2 at 300 K

Band	IR band wavenumber (cm^{-1})	Ref.
ν(CH), crotonaldehyde	3023	27, 30
$\nu(CH_3)$	2968, 2931, 2876	22
ν(C=O), Pt–CO (linear)	2041	7, 8, 15
ν(C=O), Pt–CO (bridging)	1818	7, 8, 15
ν(C=O), acyl	1680	22, 23
ν(C=O), crotonaldehyde	1655	27, 30
ν(C=C), crotonaldehyde	1628	27, 30
δ(OH), water	1630	31
ν_a(COO), acetate	1550	10
ν_s(COO), acetate	1442	10
$\delta(CH_3)$	1383	
ν(C–C), $\rho(CH_3)$	1169, 1141	27, 30

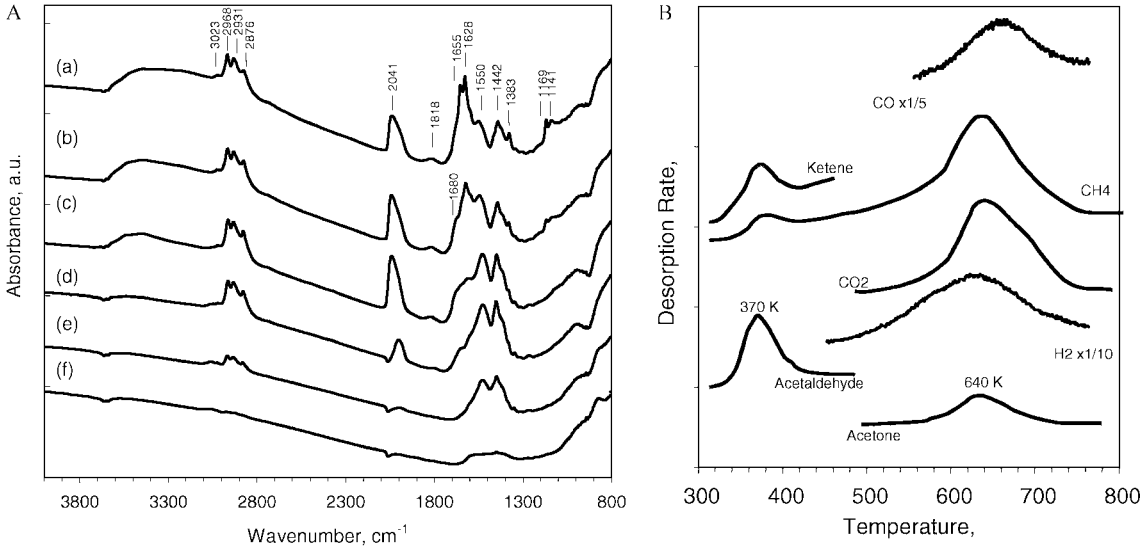

FIG. 5. (A) DRIFT spectra of species on Pt/TiO_2 (HTR) following acetaldehyde adsorption at 300 K and heating in Ar to (a) 300, (b) 373, (c) 473, (d) 573, (e) 673, and (f) 773 K. (B) TPD spectra following acetaldehyde adsorption on Pt/TiO_2 (HTR) at 300 K.

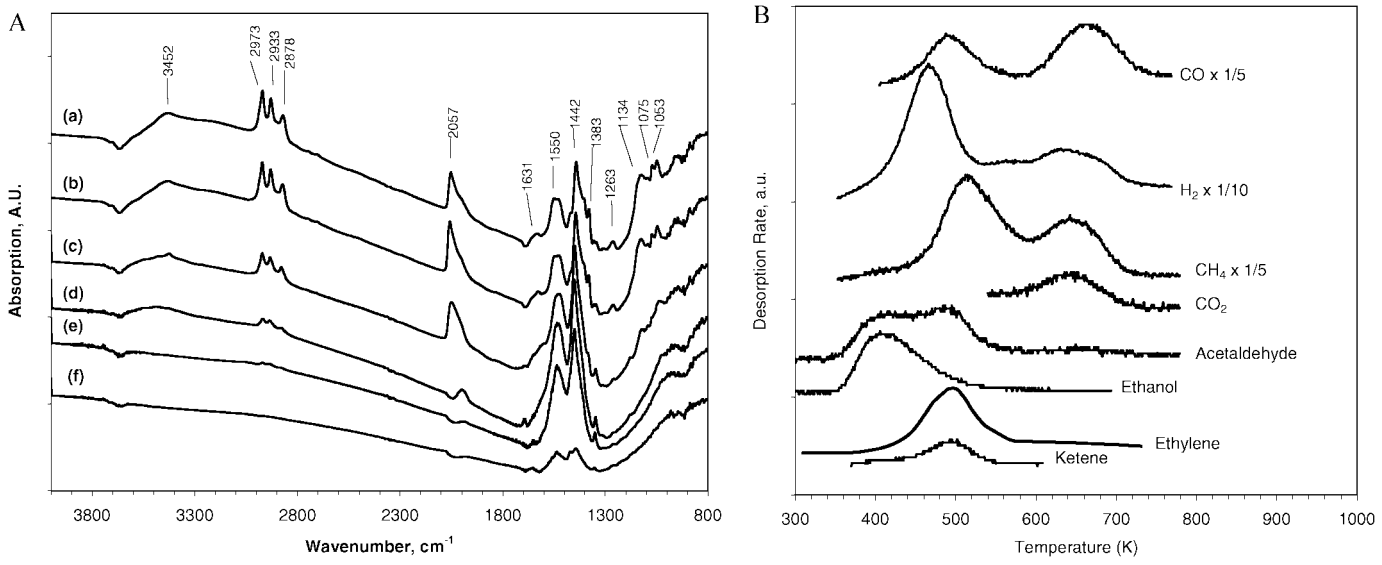

FIG. 6. (A) DRIFT spectra of species on Pt/TiO_2 (HTR) following ethanol adsorption at 300 K and heating in Ar to (a) 300, (b) 373, (c) 473, (d) 573, (e) 673, and (f) 773 K. (B) TPD spectra following ethanol adsorption of Pt/TiO_2 (HTR) at 300 K.

catalyst surface was detected during the TPD run, which was probably due to decomposition during the experiment.

DRIFTS and TPD of Ethanol on Pt/TiO_2 (HTR)

Adsorption of ethanol on Pt/TiO_2 produced an IR spectrum that was indicative of dissociative adsorption of ethanol on TiO_2 to form ethoxy and acetate species, as shown in Fig. 6A. CO was also formed as result of ethanol decarbonylation on the catalyst, as characterized by an IR band at 2057 cm^{-1}. The presence of surface ethoxy species was characterized by IR bands at 2973, 2933, and 2878 cm^{-1} for ν(C–H), and 1134 cm^{-1}, as well as a doublet, at 1053 and 1075 cm^{-1}, for ν(C–O). A surface acetate species is indicated by IR bands at 1550 cm^{-1} and 1442 cm^{-1} for ν_a(COO) and ν_s(COO), respectively. Both ethoxy and acetate species were formed on the oxide support surfaces, as they were also observed after ethanol adsorption on pure TiO_2. The complete band assignments are listed in Table 4. Stepwise heating of the catalyst to 773 K (Fig. 6A) showed that the ethoxy species remained on the surface up to 473 K, while acetate was still present on the catalyst up to 773 K. The intensity of the band at 2057 cm^{-1} (CO adsorbed on Pt) increased after heating to 373 K and then decreased upon subsequent heating, with the greatest change occurring between 473 and 573 K.

TPD runs with this catalyst showed three groups of peaks, at 400 K, between 470 and 520 K, and near 660 K, as shown in Fig. 6B, which are indicative of separate reaction/decomposition pathways associated with the surface species detected using DRIFTS. The IR spectra of ethanol adsorbed on Pt/TiO_2 suggest that there are two types of ethoxy species present on the surface giving rise to two sets of infrared bands corresponding to ν(C–O)—one at 1134 cm^{-1} and the other present as a doublet, at 1075 and 1053 cm^{-1}. This observation is consistent with results reported previously by Gamble *et al.,* who associated the former peak to an ethoxy species bound to surface Ti atoms and the latter set to the species bound at "bridging oxygen" lattice vacancies at the surface (33). Ethanol, which was produced at 400 K in the TPD experiment, was the result of recombination of the former ethoxy moiety with adsorbed hydrogen. The other ethoxy species decomposed at higher temperatures near 500 K to produce acetaldehyde, ethylene, ketene, and CH_4. The process by which acetaldehyde was produced in the TPD run is reaction limited because IR bands corresponding to adsorbed acetaldehyde were not

TABLE 4

Vibrational Assignments for Surface Species Following Ethanol Adsorption on Pt/TiO_2 at 300 K

Band	IR band wavenumber (cm^{-1})	Ref.
ν(OH)	3452	34
$\nu(CH_3)$	2973	
	2933	
	2878	
ν(C=O), Pt–CO (linear)	2057	7, 8, 15
δ(OH), water	1630	33, 34
ν_a(COO), acetate	1550	
ν_s(COO), acetate	1442	
$\delta(CH_3)$	1383	
ν(C–O), ethoxide	1263	
ν(C–C)	1134	
ν(C–O), ethoxide	1075	
	1053	

observed with DRIFTS. The low-temperature H_2 and CO peaks resulted from desorption of adsorbed hydrogen and CO formed by decarbonylation of ethanol occurring on the Pt surface, and CO desorption at this temperature is consistent with the disappearance of the 2057 cm^{-1} IR band shown in Fig. 6A. CH_4, CO, CO_2, H_2, and traces of ethylene and acetaldehyde were the result of decomposition of surface acetate species at 640 K.

DRIFTS and TPR of Acetic Acid on Pt/TiO_2

TPR experiments were conducted to examine the reactivity of acyl and acetate species with hydrogen, and Fig. 7B shows the TPR spectra for acyl and acetate species on the Pt/TiO_2 (HTR) catalyst. Desorption peaks were obtained for acetic acid at 460 and 530 K, for ethanol at 490 K, and for acetaldehyde, ethylene, CO, CH_4, and CO_2 at 530 K, and a second peak for CH_4 occurred at 573 K. Acetone and ketene were not detected. In addition to having acetic acid desorb at 460 K and ethanol desorb at 490 K, the desorption peaks for acetaldehyde, ethylene, CO, CH_4, and CO_2 were at much lower temperatures than those obtained in the TPD experiments. These differences in both the products and the peak temperatures confirm the expected reactions between hydrogen and the adsorbed acyl and acetate species.

Figure 7A shows DRIFT spectra of species adsorbed on Pt/TiO_2 (HTR) heated stepwise in flowing hydrogen. Disappearance of the band at 1680 cm^{-1} is concomitant with ethanol desorption and suggests that acyl species are the precursor to ethanol. The bidentate species, characterized by bands at 1540 and 1450 cm^{-1}, disappears almost completely upon heating to 573 K, which suggests acetaldehyde, ethylene, CO, CH_4, and CO_2 can result from acetate hydrogenation and/or the decomposition of its products. Molecular acetic acid is more likely to result from acetate species than acyl species because the recombination of the former group with a hydrogen atom directly forms an acetic acid molecule, and the two desorption peaks for acetic acid could indicate two different acetate species with respect to their recombination activity with hydrogen.

DISCUSSION

Following adsorption on catalyst surfaces, acetic acid can be present in molecular form but can also dissociate to form acyl (3) or acetate species (2, 16, 32, 35–37). Acetic acid adsorbs molecularly on the surface either by bonding to a metal cation or by hydrogen bonding with a surface hydroxyl group. In the catalyst systems studied here, adsorbed molecular acetic acid, acyl, and acetate species were identified. The DRIFTS and TPD results show that acetic acid was found only on titania and silica surfaces. Acetic acid adsorbed on titania is very weakly bound, as it exists only in the presence of vapor-phase acetic acid, and it interacts weakly with a Ti cation rather than by hydrogen bonding with a surface hydroxyl group. Silica, on the other hand, interacts more strongly with acetic acid through its surface hydroxyl groups. It appears that acetic acid desorbs from the silica surface molecularly with a peak at 420 K and the desorption continues at higher temperatures, which is most likely a result of a recombination reaction between hydrogen and silyl esters, as shown by the TPD studies. Acetate was readily formed during acetic acid adsorption on titania and Pt surfaces, but not on silica. Two forms of dissociated acetic acid were identified on titania, namely acyl and bidentate

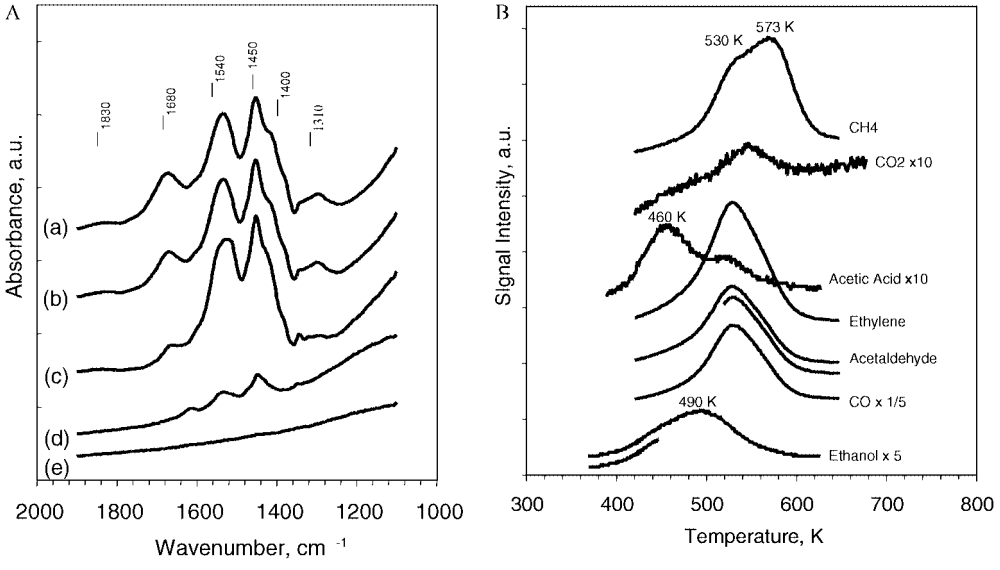

FIG. 7. (A) DRIFT spectra of species on Pt/TiO_2 (HTR) following acetic acid adsorption at 300 K and heating in H_2 to (a) 300, (b) 373, (c) 473, (d) 573, and (e) 673 K. (B) TPR spectra following acetic acid adsorption on Pt/TiO_2 (HTR) at 300 K.

acetate. The acyl species, which was found at higher surface coverages on unreduced and LTR titania surfaces, appeared to be thermally less stable than the bidentate species, and this acyl species decomposed to ketene, as evidenced by the TPD of acetic acid adsorbed on the Pt/TiO_2 (LTR) catalyst.

On the basis of the DRIFTS studies, acetic acid adsorption on Pt appears to lead to decarbonylation, which gives adsorbed CO on the Pt surface. The DRIFT spectra of acetic acid adsorbed on a highly dispersed Pt/SiO_2 catalyst also indicated the presence of acetate on Pt surfaces. Avery showed, using electron energy loss spectroscopy, that acetic acid dissociates on Pt, even below room temperature, i.e., at 225 K on Pt(111), to form an acetate species (38). Thermal decomposition of acetate on Pt already occurs at 300 K to leave adsorbed CO, characterized by infrared bands at 2050 cm^{-1} and 1838 cm^{-1}, which are associated with linear and bridged-bonded CO stretching frequencies (14). Although the decomposition is typically complete at 380 K (38), the CO desorption peak typically occurs around 450 K (39), which implies that CO desorption is surface-desorption limited rather than surface-reaction limited.

The following steps summarize acetic acid adsorption on the titania surface of Pt/TiO_2 catalyst systems to form acetate and acyl species:

$$CH_3COOH_{(g)} \rightarrow CH_3COOH_{(ad)}, \quad [1]$$

$$CH_3COOH_{(ad)} \rightarrow CH_3COO_{(ad)} + H_{(ad)}, \quad [2]$$

and

$$CH_3COOH_{(ad)} \rightarrow CH_3CO_{(ad)} + OH_{(ad)}. \quad [3]$$

No assumption is made whether the dissociative steps occur on the same type of sites or not, but the relative intensities of the IR bands corresponding to acyl and acetate species varied with different extents of titania surface reduction. Furthermore, as mentioned earlier, acyl species are adsorbed more weakly on the surface and are observed only below 573 K, whereas surface acetate species are readily formed on all titania surfaces and are shown to be very stable. Therefore, it is very likely that there are two different types of sites involved in the formation of acyl and acetate species from acetic acid.

Decomposition of acyl species produced ketene in the TPD runs, but acyl species can also react with surface lattice oxygen to form acetate, which increased the intensity of the IR band for acetate upon heating, as displayed in Figs. 2A and 3A. The conversion of an acyl species to form an acetate species can be depicted by the step

$$CH_3CO_{(ad)} + O_{(l)} \rightarrow CH_3COO_{(ad)}, \quad [4]$$

where $O_{(l)}$ designates a lattice oxygen atom. Surface acetate species can decompose following reaction pathways postulated by Kim and Barteau to produce acetone, ketene, ethylene, acetaldehyde, CH_4, CO_2, CO, and H_2 (37). These reactions occur at 600–673 K, as indicated by the TPD runs.

Acetic acid can dissociate readily on a Pt surface to form acetate, which in turn can dissociate further at temperatures as low as 225 K to leave adsorbed CO on the surface, as shown by Vajo *et al.* (40). At 300 K acetate decomposition is sufficiently rapid so that adsorbed CO can be detected in the DRIFTS spectrum immediately following acetic acid adsorption.

When acetic acid was adsorbed on the Pt/SiO_2 catalysts, extensive acetate decomposition on Pt occurred, as indicated by the IR band at 2085 cm^{-1} for adsorbed CO. There are two types of surface hydroxyl groups on a silica surface, namely free and bound OH groups (41). A reduction treatment can remove most of the bound OH groups, which are more susceptible to dehydroxylation than the free (isolated) OH groups, thus leaving the latter intact on the surface. As free OH groups are generally involved in more specific and stronger adsorption, acetic acid interacting with these hydroxyl groups might be expected to produce a more thermally stable form of adsorbed acetic acid, and this species desorbed molecularly with a maximum rate at 420 K. Some of the more strongly bound acetic acid would desorb at higher temperatures and could adsorb on the Pt to undergo decarbonylation and produce methane at 500 K. Desorption products such as ethylene, CH_4, CO, and CO_2 are the result of the decomposition of silyl esters around 600 K, because silyl esters ($\text{Si–O–}\overset{\overset{O}{\|}}{C}\text{–CH}_3$, for example) were the principal species remaining on the surface.

Both acyl and bidentate acetate species have been proposed as active intermediates because they exist in sizable concentrations under acetic acid reduction conditions. Based on these new spectroscopic results, molecularly adsorbed acetic acid does not appear to be an active intermediate to which H atoms are directly added, as proposed earlier (1), and silyl esters on Pt/SiO_2 are also excluded as reactive intermediates because neither TPD nor TPR of these species indicated any reactivity to form reduction products, in agreement with steady-state activity behavior (1). An important question, then, is whether acetate or acyl species are participating in the catalytic cycle for the initial hydrogenolysis reaction.

Acetate formation is closely related to the presence of acetaldehyde and ethanol because acetate was a commonly observed surface species after their adsorption on Pt/TiO_2. Furthermore, IR studies previously reported in the literature (2, 4), plus the IR spectra obtained in this study (26), show that active catalysts have one trait in common, i.e., they all form surface acetate species upon adsorption of acetic acid; thus, it might be logical to assume that acetate is an active surface intermediate. The TPD results, however, show that these acetate species are very strongly adsorbed and decompose at 615 K, which is far above the steady-state hydrogenation reaction temperatures (1). The acyl species, on the other hand, are less stable than the acetate and decomposes to ketene at 573 K; thus, based on

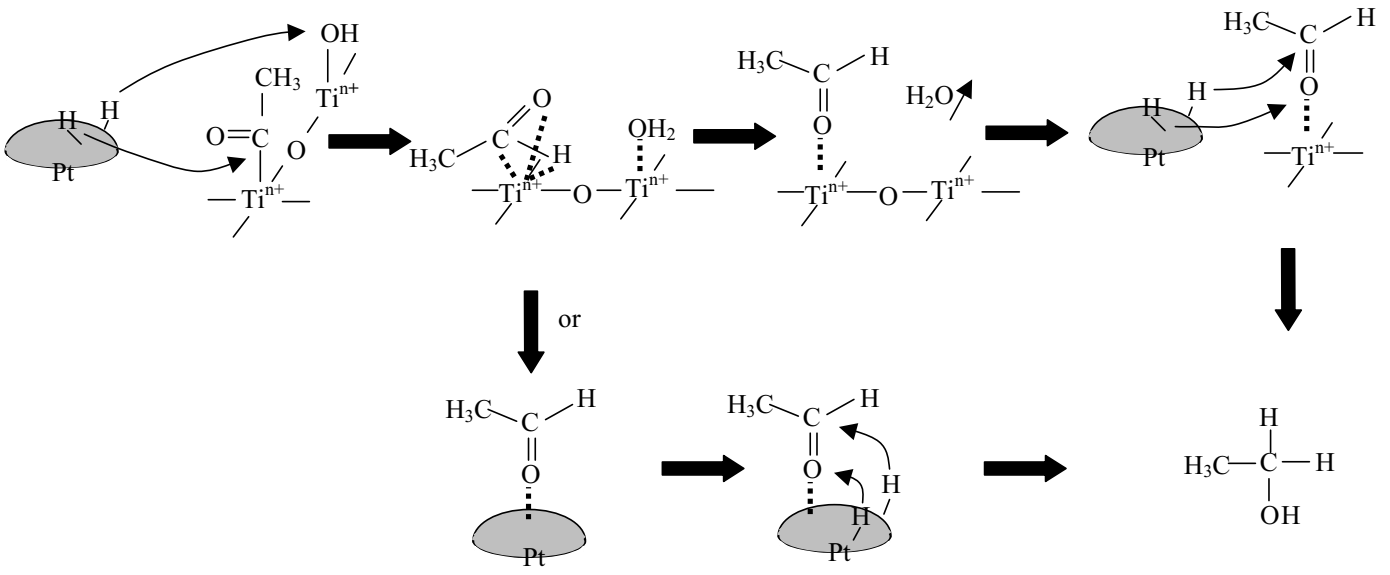

FIG. 8. Main reaction pathways on Pt/TiO_2 at steady-state reaction conditions.

the thermal stability alone, it is expected that this species would be more likely to participate in the hydrogenation catalytic cycle than the acetate.

The TPR experiments showed that both acyl and acetate are reactive toward hydrogen with the acyl species associated with the formation of acetaldehyde and ethanol. Because ethanol was produced in the TPR runs at the temperatures used for steady-state conditions (1), it is proposed here that below 500 K acyl species play a predominant role in acetic acid reduction by H_2 on Pt/TiO_2. As depicted in Fig. 8, dissociative adsorption of acetic acid on a titania site in the interfacial region produces an acyl species which can add a hydrogen atom to form adsorbed acetaldehyde. This species then either desorbs or undergoes further hydrogenation to ethanol; in the case of Pt/TiO_2, acetaldehyde is more likely to undergo further hydrogenation than to desorb. A similar mechanism has been used to explain the formation of C_2-oxygenates, i.e., acetaldehyde and ethanol, during CO hydrogenation over Rh catalysts (17, 18).

After a reduction treatment, a titania surface is comprised of Ti^{4+}, Ti^{3+}, and possibly Ti^{2+} centers with 0, 1, and 2 coordination vacancies, respectively (42–44). Edges and corners obviously contain cationic centers with higher coordinative unsaturation. An ESR study by Huizinga and Prins indicated that a HTR step results in a higher concentration of Ti^{3+}, with the Ti^{3+}/Ti^{4+} ratio being one to two orders of magnitude higher than that of a catalyst subjected to a LTR step (45). It is interesting that the surface acyl concentration decreases with an increasing degree of reduction of the titania surface, as evidenced by the DRIFT spectra of acetic acid adsorption on the LTR and HTR catalysts. Unfortunately, there is not enough information at this point to establish a relationship between surface acyl formation and the electronic state of a Ti cation; however, the importance of coordination vacancies for dissociating acetic acid on oxide surfaces suggests that a coordinatively unsaturated Ti^{n+} center is the likely candidate for the adsorption site (44). The fact that the turnover number on the HTR catalyst is seven to eight times higher than that on the LTR catalyst attests to the significance of the interfacial sites for the reaction because more of these sites are expected to exist on the surface of the former.

Reduction of surface acetate species can also lead to acetaldehyde, but higher temperatures are required. Because the reaction on Pt/TiO_2 occurs readily at temperatures below 500 K, it is reasonable to assume that surface acetate does not participate in the reaction under these conditions, but merely exists as a spectator species. A previous claim, which invoked acetate as the active intermediate, could still be valid because the reaction in this case was conducted on oxide surfaces above 500 K (2). The high-temperature requirement is attributed to the fact that oxides are only capable of dissociating and activating hydrogen at a meaningful rate at elevated temperatures. When a metal is dispersed on an oxide, such as Pt/TiO_2, it can activate hydrogen, which is why hydrogenation activity can be readily obtained at lower temperatures than those used with the oxide-only catalysts. Metals alone, however, are unfavorable because acetic acid can decarbonylate on these surfaces before undergoing reduction to acetaldehyde; therefore, the best catalyst systems are those that provide sites for activating hydrogen and yet do not create a significant amount of decomposition products. The presence of acyl species on the oxide coupled with sites that can chemisorb H_2 and furnish hydrogen atoms is instrumental in allowing the reaction to occur at low temperatures. However, it must be pointed out

that thermodynamics indicate that acetaldehyde, which is the first reduction product, can readily be converted into ethanol.

The kinetics of this reaction can still be described by incorporating this new spectroscopic information into the series of elementary steps proposed in our previous study (1). The model is simplified to include oxide sites only in the interfacial region, so that dissociated hydrogen is readily available. Then a surface acyl species, rather than molecular acetic acid, is assumed to be a predominant reaction intermediate, and this acyl species is included along with molecular acetic acid in the site balance on the oxide surface. All other aspects of the previous model remain the same; therefore, the catalytic cycle is now represented by the following sequence of elementary steps:

$$H_{2(g)} + 2^* \overset{K_{H_2}}{\rightleftharpoons} 2H^*, \quad [5]$$

$$CH_3COOH_{(g)} + 2^* \overset{K_{Ac}}{\rightleftharpoons} CH_3COO^* + H^*, \quad [6]$$

$$CH_3COOH_{(g)} + S \overset{K_A}{\rightleftharpoons} CH_3COOH\text{–}S, \quad [7]$$

$$CH_3COOH\text{–}S \overset{K_{Acy}}{\rightleftharpoons} CH_3CO\text{–}S\text{–}OH, \quad [8]$$

$$CH_3CO\text{–}S\text{–}OH + H^* \overset{k_1}{\rightarrow} CH_3CHO\text{–}S\text{–}OH + ^*, \quad [9]$$

$$CH_3CHO\text{–}S\text{–}OH + H^* \overset{k_2}{\rightarrow} CH_3CHO\text{–}S + ^* + H_2O_{(g)}, \quad [10]$$

$$CH_3CHO\text{–}S \underset{k_{-3}}{\overset{k_3}{\rightleftharpoons}} CH_3CHO_{(g)} + S, \quad [11]$$

$$CH_3CHO\text{–}S + H^* \overset{k_4}{\rightarrow} CH_3CH_2O\text{–}S + ^*, \quad [12]$$

$$CH_3CH_2O\text{–}S + H^* \overset{k_5}{\rightarrow} CH_3CH_2OH\text{–}S + ^*, \quad [13]$$

$$CH_3CH_2OH\text{–}S \underset{k_{-6}}{\overset{k_6}{\rightleftharpoons}} CH_3CH_2OH_{(g)} + S, \quad [14]$$

$$CH_3CH_2OH\text{–}S + H^* \overset{k_7}{\rightarrow} CH_3CH_2OH_2\text{–}S + ^*, \quad [15]$$

$$CH_3CH_2OH_2\text{–}S + H^* \overset{k_8}{\rightarrow} CH_3CH_3\text{–}S + ^* + H_2O_{(g)}, \quad [16]$$

$$CH_3CH_3\text{–}S \underset{k_{-9}}{\overset{k_9}{\rightleftharpoons}} CH_3CH_{3(g)} + S. \quad [17]$$

By applying the steady-state approximation to the surface intermediate concentrations (1), it can be easily shown that the rate of disappearance of acetic acid to form reduction products is

$$r_{HOAc} = k_1\theta_{Acy}\theta_H, \quad [18]$$

where the subscripts Acy and H refer to the surface acyl species ($CH_3\overset{O}{\overset{\|}{C}}\text{–S–OH}$) adsorbed on an oxide site, S (which can involve more than one atom), and a hydrogen atom adsorbed on a metal site, *, respectively. The total number of active sites is incorporated in k_1. If reactions [5]–[8] are quasiequilibrated, it can be readily shown that

$$r_{HOAc} = k_1K_{Acy}K_AK_{H_2}^{1/2}P_AP_{H_2}^{1/2}\theta_s\theta_*, \quad [19]$$

where θ_s and θ_* represent the fraction of empty sites on the oxide and metal surfaces, respectively.

The assumption of quasiequilibrated H_2 and acetic acid adsorption on * sites, as depicted by steps [5] and [6], to give a nearly saturated Pt surface covered by H atoms and acetate species as the principal surface intermediates yields the following expression for the surface fraction of empty sites, θ_*:

$$\theta_* = \frac{1}{\left(K_{H_2}^{1/2}P_{H_2}^{1/2} + K_{Ac}P_A/K_{H_2}^{1/2}P_{H_2}^{1/2}\right)}. \quad [20]$$

Quasiequilibrated acetic acid adsorption and acyl species formation on S sites (reaction steps [7] and [8]) give

$$\theta_S = \frac{1}{(1 + K_AP_A + K_{Acy}K_AP_A)} = \frac{1}{(1 + K_A(1 + K_{Acy})P_A)} \quad [21]$$

based on the DRIFT spectra showing that both molecular acetic acid and acyl species existed on the titania surface sites. Because of this information and the low conversions used, only acetic acid and acyl species are included in the site balance. Substituting the last two equations into Eq. [19] gives the final rate expression,

$$r_{HOAc} = \frac{k_1K_{Acy}K_AK_{H_2}^{1/2}P_AP_{H_2}^{1/2}}{\left(K_{H_2}^{1/2}P_{H_2}^{1/2} + K_{Ac}P_A/K_{H_2}^{1/2}P_{H_2}^{1/2}\right)(1 + K_A(1 + K_{Acy})P_A)} = \frac{k_1'P_AP_{H_2}^{1/2}}{\left(K_2P_{H_2}^{1/2} + K_3P_A/P_{H_2}^{1/2}\right)(1 + K_4P_A)}, \quad [22]$$

where $k_1' = k_1K_{Acy}K_AK_{H_2}^{1/2}$, $K_2 = K_{H_2}^{1/2}$, $K_3 = K_{Ac}/K_{H_2}^{1/2}$, and $K_4 = K_A(1 + K_{Acy})$. With these four parameters, this equation was fitted to the experimental data obtained from the Arrhenius and the partial pressure runs with the 0.69% Pt/TiO_2 (HTR) and 2.01% Pt/TiO_2 (LTR) catalysts using a least-squares nonlinear optimization method. The iteration process was initiated with a number of sets of initial values, each with reasonable initial values for k_1', K_2, K_3, and K_4, and it continued until optimum values were obtained at one temperature. The rate expression was fitted to experimental data at three temperatures to obtain three separate sets of values for k_1', K_2, K_3, and K_4, which are listed in Table 5 along with the values of the equilibrium adsorption constants, K_i, derived from these values. The fit of Eq. [22] to these data is identical to that obtained with the rate expression used previously (1), as shown in Fig. 9. The standard enthalpy and entropy of adsorption can be obtained from Arrhenius plots of the equilibrium adsorption constants, as

TABLE 5

Optimized Rate Parameters for Pt/TiO_2 Catalysts[a]

Catalyst	$k_1' \times 10^{-4}$ (μmol/s · g of cat · $atm^{3/2}$)	$K_2 \times 10^{-2}$ ($atm^{-1/2}$)	$K_3 \times 10^{-4}$ ($atm^{-1/2}$)	K_4 (atm^{-1})	$K_{H_2} \times 10^{-5}$ (atm^{-1})	$K_{Ac} \times 10^{-7}$ (atm^{-1})
0.69% Pt/TiO_2 (HTR)						
Temp (K) = 437	6.5	22.5	7.5	10.9	50.8	17.0
460	6.8	8.7	5.4	4.4	7.6	4.7
470	8.5	7.0	4.7	5.5	4.8	3.4
2.01% Pt/TiO_2 (LTR)						
Temp (K) = 422	4.7	13.2	6.7	4.3	17.4	8.9
445	6.8	7.8	5.4	3.3	6.1	4.2
465	6.0	2.6	3.6	0.4	0.7	0.9

[a] In Eq. [22].

shown in Fig. 10, and Table 6 lists the corresponding values obtained for K_{H_2} and K_{Ac} while $K_A(1+K_{Acy})$ is maintained as a single lumped parameter expressed as

$$K_A(1 + K_{Acy}) = \exp(\alpha/R - \beta/RT), \qquad [23]$$

where α and β are comparable values that can be extracted from the intercept and the slope of the Arrhenius plot of this term. Essentially identical values are obtained for the enthalpies of H_2 adsorption as well as the entropies of H_2 adsorption on Pt surfaces in the Pt/TiO_2 (LTR) and Pt/TiO_2 (HTR) catalysts, and the thermodynamic values for acetic acid on Pt dispersed in either TiO_2 catalyst are also very similar, as one might anticipate. The enthalpy values for H_2 are similar to those reported for initial adsorption on clean Pt surfaces (46), while the two entropies of adsorption are at the high end of acceptable values and imply loss of all entropy (47, 48). These values are higher than expected, but their uncertainty is also high. Unfortunately, no heat of adsorption for acetic acid on Pt was found in the literature. In contrast, the values for α and β are significantly different between these catalysts, indicating different thermodynamic behavior regarding acetic acid adsorption and acyl formation on the titania surface after an LTR or an HTR pretreatment. Depending on the relative surface coverages of adsorbed acetic acid and acyl species, these values can provide

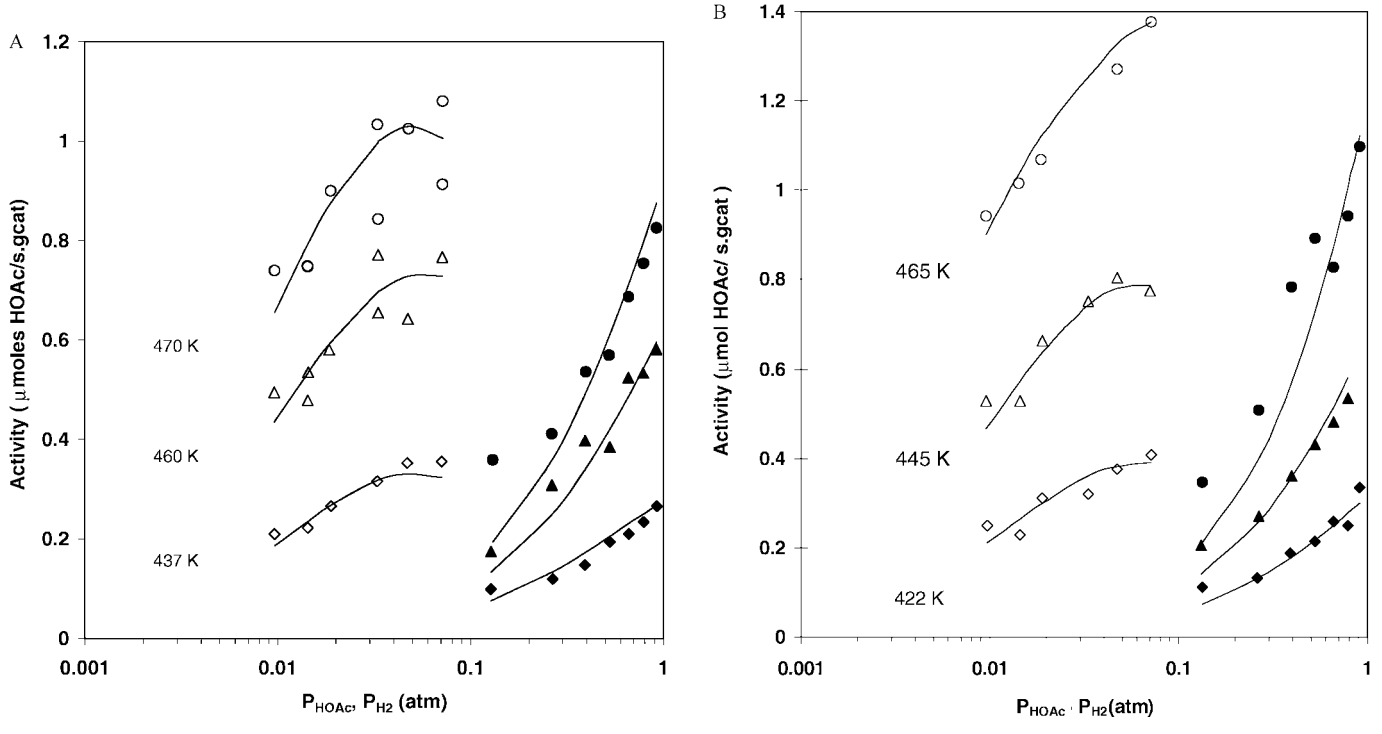

FIG. 9. Reduction activity over Pt/TiO_2 catalysts versus acetic acid and hydrogen partial pressures. Solid lines indicate the optimum fit obtained by fitting Eq. [22] to the experimental data points: (A) 0.69% Pt/TiO_2 (HTR) at 437, 460, and 470 K; (B) 2.01% Pt/TiO_2 (LTR) at 422, 445, and 465 K.

TABLE 6

Enthalpies and Entropies of Adsorption from Rate Parameters with 90% Confidence Limits[a]

Catalyst	K_{H_2}		K_{Ac}		$K_A(1+K_{Acy})^b$	
	ΔH^0 (kcal/mol)	ΔS^0 (cal/mol · K)	ΔH^0 (kcal/mol)	ΔS^0 (cal/mol · K)	β (kcal/mol)	α (cal/mol · K)
0.69% Pt/TiO_2 (HTR)	-30 ± 14	-37 ± 30	-21 ± 5	-10 ± 12	-10 ± 34	-18 ± 75
2.01% Pt/TiO_2 (LTR)	-29 ± 50	-39 ± 114	-20 ± 34	-11 ± 77	-22 ± 72	-47 ± 163

[a] Standard state, 1 atm.
[b] $K_A(1+K_{Acy}) = \exp(\alpha/R - \beta/RT)$.

insight about acetic acid adsorption on titania. If the surface coverage of molecular acetic acid were significantly larger than that of the acyl species, i.e., $\theta_A \gg \theta_{Acy}$, Eq. [23] reduces to

$$\exp(\alpha/R - \beta/RT) = K_A = \exp\left(\Delta S^0_A/R - \Delta H^0_A/RT\right), \quad [24]$$

where ΔS^0_A and ΔH^0_A represent the entropy and enthalpy of molecular acetic acid adsorption on titania, as depicted by Eq. [7]. Alternatively, if the opposite were true, i.e., $\theta_{Acy} \gg \theta_A$, Eq. [23] reduces to

$$\exp(\alpha/R - \beta/RT) = K_A K_{Acy} = \exp\left(\Delta S^0_{AAcy}/R - \Delta H^0_{AAcy}/RT\right) \quad [25]$$

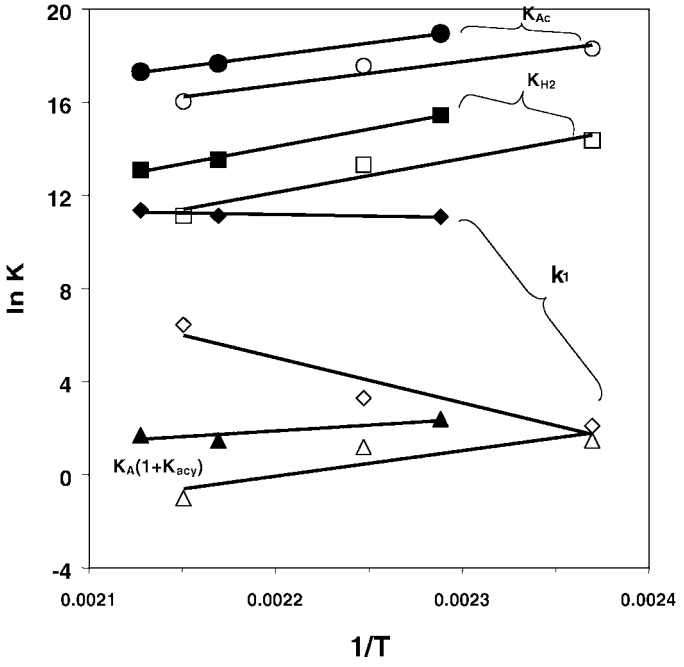

FIG. 10. Arrhenius plots of optimized rate parameters from Table 5: 0.69% Pt/TiO_2 (HTR), filled symbols; 2.01% Pt/TiO_2 (LTR), open symbols.

and ΔS^0_{AAcy} and ΔH^0_{AAcy} now represent the respective entropy and enthalpy of acetic acid adsorption to form an acyl species. If the fractional surface coverages of both species are comparable, α and β then represent a composite of these ΔS^0 and ΔH^0 values.

For either limiting case, both the enthalpy and entropy of adsorption must be negative and satisfy certain thermodynamic criteria (47, 48), which they do. The reaction model forwarded here proposes that surface acyl species, rather than acetic acid, is the catalytically significant species, at least under the reaction conditions used in this study, and DRIFT spectra of acetic acid adsorbed on either the LTR or the HTR catalyst indicate that the surface coverage of acyl species is far higher than that of molecular acetic acid. Consequently, Eq. [25] appears to be more appropriate for these catalysts, which renders α and β as the respective ΔS^0 and ΔH^0 values for dissociative acetic acid adsorption on titania to form a surface acyl species.

SUMMARY

Molecular acetic acid, acyl species, and bidentate acetate species on titania as well as CO adsorbed on Pt are surface species detected by DRIFTS and TPD following acetic acid adsorption on Pt/TiO_2 catalysts. Adsorbed CO on Pt resulted from the decarbonylation of acetic acid. The temperature-programmed reaction of these surface species with hydrogen provided evidence that reduction of acetic acid by hydrogen on Pt/TiO_2 occurs primarily via a surface reaction between adsorbed hydrogen atoms and a surface acyl species rather than molecular acetic acid or an acetate species, and this serves as the major route to produce acetaldehyde and, subsequently, ethanol. The very stable nature of acetate at the steady-state reaction conditions used here discounts it as a principal intermediate; however, at temperatures above 500 K, acetate may become an active intermediate in the surface hydrogenolysis reaction to produce acetaldehyde. The absence of surface acyl species and a stable acetate species on Pt/SiO_2 account for the lack of any acetic acid reduction activity on this catalyst, and only decomposition products were obtained. Based on these new spectroscopic results about surface species, a reaction

mechanism proposed earlier was modified to incorporate this information, and the resulting rate expression gave a fit to the data identical to that obtained previously and it also possessed thermodynamically consistent rate parameters.

ACKNOWLEDGMENT

This study was sponsored by the DOE, Division of Basic Energy Sciences, via Grant DE-FO2-84ER13276.

REFERENCES

1. Rachmady, W., and Vannice, M. A., *J. Catal.* **192**, 322 (2000).
2. Pei, Z.-F., and Ponec, V., *Appl. Surf. Sci.* **103**, 171 (1996).
3. Natal-Santiago, M. A., Sanchez-Castillo, M. A., Cortright, R. D., and Dumesic, J. A., *J. Catal.* **193**, 16 (2000).
4. Pestman, R., Ph.D. thesis. Leiden University, The Netherlands, 1995.
5. Mao, C.-F., and Vannice, M. A., *J. Catal.* **154**, 230 (1995).
6. Gorte, R. J., *J. Catal.* **75**, 164 (1982).
7. Vannice, M. A., Twu, C. C., and Moon, S. H., *J. Catal.* **79**, 70 (1983).
8. Tanaka, K., and White, J. M., *J. Catal.* **79**, 81 (1983).
9. Tauster, S. J., Fung, S. C., and Garten, R. L., *J. Am. Chem. Soc.* **100**, 170 (1978).
10. Nakamoto, K., "Infrared and Raman Spectra of Inorganic and Coordination Compounds," 4th ed. Wiley, New York, 1986.
11. Maréchal, Y., *J. Chem. Phys.* **87**, 6344 (1987).
12. Haurie, M., and Novak, A., *Spectrochim. Acta* **21**, 1217 (1965).
13. Haurie, M., and Novak, A., *J. Chim. Phys.* **62**, 146 (1965).
14. Ito, K., and Bernstein, H. J., *Can. J. Chem.* **34**, 170 (1956).
15. Nguyen, T. T., and Sheppard, N., *in* "Advances in Infrared and Raman Spectroscopy" (R. E. Hester and R. H. J. Clark, Eds.), Vol. 5. p. 15. Heyden, London, 1978.
16. Jackson, S. D., Kelly, G. J., and Lennon, D., *React. Kinet. Catal. Lett.* **70**, 207 (2000).
17. Underwood, R. P., and Bell, A. T., *J. Catal.* **111**, 325 (1988).
18. Fukushima, T., Arakawa, H., and Ichikawa, M., *J. Chem. Soc., Chem. Commun.* 729 (1985).
19. Deeming, A. J., and Shaw, B. L., *J. Chem. Soc. A* 597 (1969).
20. Chini, P., Martinengo, S., and Garleshelli, G., *J. Chem. Soc., Chem. Commun.* 709 (1972).
21. Chatt, G., Johnson, N. P., and Shaw, B. L., *J. Chem. Soc. A* 604 (1967).
22. Demri, D., Hindermann, J.-P., Diagne, C., and Kienneman, A., *J. Chem. Soc., Faraday Trans.* **90**, 501 (1994).
23. Adams, D. M., and Booth, G., *J. Chem. Soc.* 1112 (1962).
24. Gao, Q., and Hemminger, J. C., *J. Electron Spectrosc. Relat. Phenom.* **54/55**, 667 (1990).
25. Gao, Q., and Hemminger, J. C., *Surf. Sci.* **248**, 45 (1991).
26. Rachmady, W., Ph.D. thesis. Pennsylvania State University, University Park 2001.
27. Rekoske, J. E., and Barteau, M. A., *Langmuir* **15**, 2061 (1999).
28. Idriss, H., Kim, K. S., and Barteau, M. A., *J. Catal.* **139**, 119 (1993).
29. Idriss, H., and Barteau, M. A., *Catal. Lett.* **40**, 147 (1996).
30. Dandekar, A., Baker, R. T. K., and Vannice, M. A., *J. Catal.* **184**, 421 (1999).
31. Little, L. H., "Infrared Spectra of Adsorbed Species." Academic Press, San Diego, 1966.
32. Thornton, E. W., and Harrison, P. G., *J. Chem. Soc. Faraday Trans. I* **71**, 2468 (1975).
33. Gamble, L., Jung, L. S., and Campbell, C. T., *Surf. Sci.* **348**, 1 (1996).
34. Hussein, G. A. M., Sheppard, N., Zaki, M. I., and Fahim, R. B., *J. Chem. Soc., Faraday Trans.* **87**, 2661 (1991).
35. Cocks, I. D., Guo, Q., Patel, R., Williams, E. M., Roman, E., and de Segovia, J. L., *Surf. Sci.* **377–379**, 135 (1997).
36. Li, Y., and Bowker, M., *J. Catal.* **142**, 630 (1993).
37. Kim, K. S., and Barteau, M. A., *Langmuir* **4**, 945 (1988).
38. Avery, N. R., *J. Vac. Sci. Technol.* **20**, 592 (1982).
39. Kawasaki, K., Kodama, T., Miki, H., and Kioka, T., *Surf. Sci.* **64**, 349 (1977).
40. Vajo, J. J., Sun, Y.-K., and Weinberg, W. H., *J. Phys. Chem.* **91**, 1153 (1987).
41. Davydov, V. Y. A., Kiselev, A. V., and Zhuravlev, L. T., *Trans. Faraday Soc.* **60**, 2254 (1963).
42. Göpel, W., Anderson, J. A., Frankel, D., Jaehnig, M., Phillips, K., Schäfer, J. A., and Rocker, G., *Surf. Sci.* **139**, 333 (1984).
43. Idriss, H., Kim, K. S., and Barteau, M. A., *Surf. Sci.* **262**, 113 (1992).
44. Barteau, M. A., *J. Vac. Sci. Technol. A* **11**, 2162 (1993).
45. Huizinga, T., and Prins, R., *J. Phys. Chem.* **85**, 2156 (1981).
46. Sen, B., Chou, P., and Vannice, M. A., *J. Catal.* **101**, 517 (1986).
47. Boudart, M., *AIChE J.* **18**, 465 (1972).
48. Vannice, M. A., Hyun, S. H., Kalpakci, B., and Liauh, W. C., *J. Catal.* **56**, 358 (1979).